energies

MDPI

Article

Rheology and Mechanical Properties of Fly Ash-Based Geopolymer Mortars with Ground Granulated Blast Furnace Slag Addition

Mateusz Sitarz, Maciej Urban and Izabela Hager *

Chair of Building Materials Engineering, Faculty of Civil Engineering, Cracow University of Technology, 31-155 Cracow, Poland; mateusz.sitarz@pk.edu.pl (M.S.); maurban@pk.edu.pl (M.U.)

* Correspondence: izabela.hager@pk.edu.pl; Tel.: +48-126-282-367

Received: 26 April 2020; Accepted: 19 May 2020; Published: 21 May 2020



Abstract: Geopolymers are less energy-demanding alternatives to Portland cement binders. The subject of geopolymer rheology has not yet been fully explored, and the available literature is limited to a narrow range of material compositions. This paper presents the rheological and mechanical response of fly-ash based geopolymer mortars. Investigations were made of the effect of different levels of ground granulated blast furnace slag (GGBFS) addition levels on the rheological properties of fresh geopolymers as well as their mechanical performances at 2, 14 and 28 days. The aim of the study was to obtain flow curves and to establish the correlation between shear stress and shear rate. The results have shown that geopolymer mortar is a pseudoplastic liquid presenting shear thinning behavior, moreover, with the increase of GGBFS content, higher material strengths were obtained and the total porosity was reduced.

Keywords: rheology; GGBFS; fly ash geopolymer; viscosity; strength; sustainability

1. Introduction

Geopolymers are considered low carbon-footprint binders because in the production phase the amount of CO_2 generated may amount to only 10% of the carbon dioxide emitted during Portland cement manufacturing [1,2]. In addition, the technological processes related to the production of geopolymers allow the use of solid waste from the industrial and energy sectors [3]. As construction materials, geopolymers show high compressive strength, great fire resistance, thermal resistance and durability in many environments [4–6]. Geopolymer binders are very often presented as alternatives to Portland cement-based materials. The available results mainly concern their chemical properties, mechanical properties, microstructure and the possibility of the potential application of the material. There is, however, little research regarding their rheological behavior. Rheological parameters are used to evaluate consistency, loss of workability, stability and pumpability [7,8]. Due to the very wide range of raw materials used in the geopolymer technology, both precursors (fly ash—FA, ground granulated blast furnace slag—GGBFS and metakaolin) and activators (sodium or potassium alkaline solution) indicate the need of complex analysis the rheology issues in geopolymer mixes. Knowledge about viscosity changes, yield strength and thixotropy as a function of time in combination with the values of the strength parameters that are obtained is extremely important especially in the context of intensively developing 3D printing technology using geopolymer material.

Fresh geopolymer paste is a solid–liquid suspension [9]. The geopolymer mix at an early stage of the reaction is a three-part composite, assuming that the air content is neglected. The first component is the aluminosilicate precursor in the form of a solid phase (e.g., GGBFS, fly ash and metakaolin) [10]. The second component is an alkaline solution containing alkalis and pre-existing silicate oligomers.

The crystalline zeolite products are formed when pure hydroxide solution is used [11] hence the use of sodium silicate solution is necessary to form amorphous geopolymeric structures. The third component is the product of the reaction between the aluminosilicate precursor and the alkaline activator. This component is the most complex and, in addition, heterogeneous even in the initial stage when the mix is well composed [12,13]. This is the most important phase affecting the mechanical properties of the geopolymer mix [14]. Due to the complex composition of the geopolymer paste, it is difficult to unequivocally identify the mechanisms affecting the rheological properties of a geopolymer mix.

Favier et al. [15] carried out a study during which each component was observed separately, and then, using scaling methods, conclusions regarding the physical and chemical properties of the geopolymeric paste were drawn. During the first stage, the geopolymer rheological properties at fresh state, when all the three components mixed together, were analyzed. The second step was to analyze the behavior of the liquid phase and solid phase separately and not taking into account the reaction product. In the last step the behavior of the reaction product was investigated. In the early stages of geopolymerization, dissolution and polymerization rates related to the H_2O/Na_2O: SiO_2/Na_2O ratios were of a major influence on the properties of the material. The mechanical properties at early age of geopolymer mixes seem not to be affected by the colloidal interactions between metakaolin grains. Al-rich gel is formed (Si/Al < 4.5) at the grain surface, within 15 min from the start of mixing. The authors of the study [15] warn against generalizations regarding the results obtained pointing at the fact that the mechanisms responsible for the of aluminosilicate gel formation at the beginning of the process depend on the type of precursor and chemical composition of the activator. When using fly ashes and GGBFS, the presence of calcium can significantly alter the chemical structure of the geopolymer system and strengthen the interfacial transition zone.

Other study carried out by Favier et al. [16] concerned the comparison between the rheology of metakaolin (MK) based geopolymer paste and the rheology of cement pastes. It was found that, from a macroscopic point of view, the geopolymer is a viscous fluid. It is characterized by very low yield stress and high viscosity. According to Flatt [17], yield stress of cement mixes is controlled by plasticizers and superplasticizers. The use of admixtures common in cement concrete technology for MK-based geopolymers does not bring the desired effects due to the almost pure viscous behavior of the material. It is possible that it can be effective in the case of precursors with calcium content, such as fly ashes or GGBFS. The viscosity of a geopolymer material is a result of the viscosity of the alkaline silicate solution. Furthermore, the chemical reactions taking place during the setting process quickly modify the rheological behavior of geopolymers [18].

The results of studies into geopolymer bonding mechanisms [19] show that the molar ratio (*MR*) of the alkaline solution plays a key role in accelerating the geopolymer hardening process. When solutions with a lower *MR* value are used, the course of the condensation reaction between Si and Al oligomers is faster, the setting time of the material is shortened and, as a result, the open time for 3D concrete printing is very short. In the case of materials used for 3D printing, it is very important to optimize the delay time between layers to ensure sufficient water content in the contact area. In the case of geopolymer mortars, the degree of cross-linking of the material mainly depends on an irreversible chemical reaction. The use of an alkaline solution with lower reactivity reduces the degree of cross-linking of the material and affects the overall strength of the resulting material.

Panda et al. [20] researched the effect of ground granulated blast furnace slag (GGBFS) or silica fume (SF) on the fresh and hardened properties of fly ash-based geopolymer mixes for 3D concrete printing. As in the case of OPC (Ordinary Portland Cement) -based mixes [21], an increase in the yield stress of geopolymers with time was observed, which is a result of the physical interaction of the particles and the chemical activation of the binder. In the case of mixes containing GGBFS, a clear increase in yield stress was observed after 20 min of mixing, which was most probably caused by accelerated setting of the mixes by the activation of GGBFS [22]. The reactivity of fly ash based geopolymers with GGBFS is much higher in ambient conditions. Furthermore, the study results

indicate a limited effect of GGBFS on the properties of fresh geopolymer pastes and a clear influence on the increase of the early age compressive strength. Moreover, the inclusion of GGBFS in the binder composition contributes to the development of a homogenous microstructure and the formation of a stronger 3-dimensional network. The addition of GGBFS does not significantly improve the rheology of the mix, but reduces the workable time of the paste. Due to the requirements regarding the setting time of the mix and the strength of the material, the amount of GGBFS used must be carefully controlled.

Other studies of geopolymer mixes [21,23] show that the rheology of geopolymers is strongly dependent on the viscous nature of the alkaline solution used, not with a particle interaction. The rheology of fresh geopolymer pastes can be controlled by dissolution and geopolymerization in the suspension system. In the case of geopolymer binders, the molar ratio of the alkaline solution used in the material synthesis process determines the ion dissolution and polymerization of fresh pastes, therefore it is the main factor affecting the rheology of the fresh geopolymer pastes.

The results of the study [24] show that a low content of sodium hydroxide decreases the fluidity of fresh geopolymer pastes. The fluidity of geopolymer pastes gradually increases together with the amount of NaOH added. High alkali content in geopolymer pastes reduces yield stress and plastic viscosity. The increase in the Si/Na ratio of the alkali activator reduces the yield stress of fresh pastes. The rate of development of yield stress increases with a decrease in the Si/Na ratio [25].

Based on the literature review, it can be concluded that the problem of the rheology of geopolymer composites is quite complex. Apart from the alkaline solution, the main factor shaping the properties of the geopolymer binder is the type of precursor used. Considering the possibility of setting material at ambient temperature and high strength values, it seems beneficial to use a blended FA-GGBFS binder. The use of this type of binder extends the application possibilities of geopolymer composites. The aim of the study was to expand knowledge in the field of rheology of blended FA/GGBFS based geopolymer mortars. Three types of mortars were prepared in which binders FA were replaced by 10 wt%, 30 wt% and 50 wt% of GGBFS. The consistency of fresh mortar was determined and the rheological properties of the mixtures were investigated using a rheometer. The kinetics of strength development and the porosity after 28 days were determined. The research results can be used to develop geopolymer technology, in particular in terms of application possibilities. One of the possible directions of application of geopolymer binders is 3D printing.

2. Materials and Methods

2.1. Materials

Siliceous fly ash (FA) produced by the Połaniec power plant, Poland, and ground granulated blast furnace slag (GGBFS) obtained from Ekocem, Poland were used in the study. The main components of this fly ash are SiO_2—52 wt% and Al_2O_3—28 wt%. In addition, the FA Połaniec contains Fe_2O_3 and a small amount of MgO, K_2O, TiO_2 and Na_2O. The total content of silicondioxide, alumina and iron (III) oxide exceeds 70 wt%. Due to its specific chemical composition, Połaniec fly ash is classified as a siliceous ash and based on the chemical analysis and according to EN 450-1:2012, this FA can be classified as type II. According to ASTM C618, the FA belongs to class F. The specific gravity of the fly ash and ground granulated blast furnace slag (GGBFS) used was 2.1 g/cm^3 and 2.9 g/cm^3, respectively. Siliceous sand (0/2 mm) was used to prepare the geopolymer mortars. The chemical composition of the FA and GGBFS can be found in Tables 1 and 2 respectively.

Table 1. X-ray fluorescence (XRF) analysis of fly ash (FA), data supplied by the manufacturer.

SiO_2	Al_2O_3	Fe_2O_3	CaO	MgO	SO_3	K_2O	Na_2O	P_2O_5	TiO_2	Mn_3O_4
52.30	28.05	6.32	3.05	1.71	0.28	2.51	0.76	0.69	1.35	0.07

Table 2. Composition of ground granulated blast furnace slag (GGBFS), data supplied by the manufacturer.

SiO_2	Al_2O_3	Fe_2O_3	CaO	MgO	SO_3	K_2O	Na_2O	Cl^-	Na_2Oeq	Blaine
39.31	7.61	1.49	43.90	4.15	0.51	0.356	0.468	0.038	0.702	3904

To prepare the solution, sodium silicate solution (Chempur, Poland, Na_2O = 11.1 wt%, SiO_2 = 27.9 wt%, H_2O = 61.0 wt%), sodium hydroxide pellets and water were used together. The prepared sodium alkaline solution was characterized by a molar ratio *MR* = 1.7. Preparation of the alkaline solution started from dissolution of NaOH pellets in water. In the next step NaOH solution was mixed with sodium silicate solution and extra water. The resulting solution was stored for 24 h prior to use.

In order to determine the effect of GGBFS on the behavior of the geopolymer mix, the content of the additive was varied. Mortars containing 10 wt%, 30 wt% and 50 wt% replacement of FA by GGBFS were analyzed. Geopolymer mortars were signed G10, G30 and G50 where the numerical value corresponds to the mass percentage content of GGBFS in binder composition. The compositions of all mortars are given in detail in Table 3. In this study the molar ratio of alkaline solution (*MR* = 1.7), sand to binder, alkaline solution to binder (FA+GGBFS) and water to binder (FA+GGBFS) ratios were set as constants. The values are shown in the Table 4. In this study no plasticizers or superplasticizers were used.

Table 3. Compositions of geopolymer mortar per $1m^{3.}$

Components	G 10 (kg/m^3)	G 30 (kg/m^3)	G 50 (kg/m^3)
Alkaline solution	337.7	342.4	347.2
Fly ash (FA)	675.4	532.6	385.8
GGBFS	75.0	228.2	385.8
Sand(0/2 mm)	1125.6	1141.2	1157.3

Table 4. Parameters of the geopolymer mortar.

Sand to Binder Ratio	Alkaline Solution to Binder (FA+GGBFS) Ratio	Water to Binder Ratio
1.5	0.45	0.30

To obtain the same volume of the mortar with a different mass of GGBFS in the composition. The content of other components has been corrected. FA and GGBFS differ in density.

The mixing of all mortars was carried out in accordance with the procedure optimized for the geopolymer by Davidovits [26], as follows.

(I) Preparation of an alkaline solution—24 h before starting the mixing. The total amount of water required in the mortar composition was added directly to the alkaline solution. Due to the exothermal character of the reaction, water evaporation was prevented during the cooling down of the alkaline solution and the container was enclosed with a lid.

(II) Paste preparation. FA with an alkaline solution was mixed first for 10 min, and then GGBFS was introduced and mixed for another 3 min.

(III) Incorporation of aggregate. Eventually, quartz sand sized 0/2 mm with a specific mass of 2.64 g/cm^3 was added and the mortar was mixed for 2 min.

2.2. Methodology

Immediately after mixing fresh geopolymer mortar samples were put into rheometer and the first measurement was performed. The start of measurement procedure was set at 200 ± 20 s after

finishing of the mixing process. Secondly, the consistency was determined (by the flow table method, following EN 1015-3 procedure). The test was set at 10 min after finishing the mixing process. Third and fourth step were rheological measurement repetition, after 15 and 25 min, respectively. Finally, the 40 mm × 40 mm × 160 mm samples were formed for hardened state tests. Mortars set at ambient temperature (T = 18 ± 2 °C, RH = 75%) in plastic molds with a lid. Additional heating was not applied. After removed from the molds, samples were stored in the same ambient conditions.

A prototype RMB-2 rotational rheometer with a helix impeller was used to determine the rheological properties [27]. It is a rheometer with a layout corresponding to the mKII setup by Tattersall and Banifill [28] with a driven external cylinder and measurement of the torque of the probe axis on a rigid beam. The external cylinder capacity was approximately 4.5 dm^3.

The equipment can be programmed for any speed–time procedure including the frequency of the data collecting during the experiment. The typical descending ramp technique was used, with a speed range from 50 to 2 rpm (0.84 ÷ 0.03 (1/s)), 11 steps, with a repetition of the highest speed at the end. The initial maximum speed was held for 20 s to obtain a proper breakdown of the structure and the following steps were held for 6 s. The flow curves were plotted in the M (Nm)—ω (1/s) units.

The physical (density) and mechanical (compressive and flexural tensile strength) properties of hardened mortars were tested over time to monitor the evolution of those properties during curing. Flexural tensile strength was performed on 40 mm × 40 mm × 160 mm specimen in three-point bedning and constant load rate of 50 N/s. The remaining mortar prisms were used for the determination of compressive strength on a hydraulic press according to the standard procedure for cement mortar with a constant load rate 2400 N/s. The tests were carried out at the age of 2, 14 and 28 days.

Furthermore, after 28 days pore size distribution was measured with mercury intrusion porosimetry (MIP). Using MIP open pores between 3.5 nm and 500 μm were detected [29] the pore size distribution and total cumulative porosity was determined and presented.

3. Results and Discussion

3.1. Effect of GGBFS Content on Fresh Mix Parameters

The consistency of the fresh mortar is given in. Table 5. The results were obtained approximately 10 min after finishing of the mixing process.

Table 5. Consistency of fresh mortar measured by the Haegermann flow table (free flow/after 15 strokes).

Mortar	G 10 (cm)	G 30 (cm)	G 50 (cm)
Flow	10/12	10/12.5	14.5/16

The results of the tests carried out in the rheometer are presented in the form of flow curves in the graphs in Figure 1.

In all presented cases the Herschel–Bulkley (see Equation(1)) shear-thinning response (i.e., $n << 1$) of the material was observed. It is a rather seldom case in concrete rheology, caused probably by the phenomena described as follows, illustrated in Figure 2. First of all, a much higher content of binder was used (c.a. 200% of typical ready-mixed concrete). It led to obtaining a much stickier paste (i.e., highly cohesive and viscous [30]). Secondly, a low maximum grain size of aggregate was used, similarly rather to mortars than to concrete. It results in yield value lowering, especially at low speeds [31]. Thirdly, consistency of the mixes (see Table 5) was low as no fluidifying admixtures was used.

$$\tau = \tau_0 + \eta \cdot \dot{\gamma}^n \quad (1)$$

where:

τ—shear stress;

τ_0—yield stress;
η—non-linear viscosity;
$\dot{\gamma}$—shear strain rate;
n—exponent (non-linearity factor; for Bingham model $n = 1$).

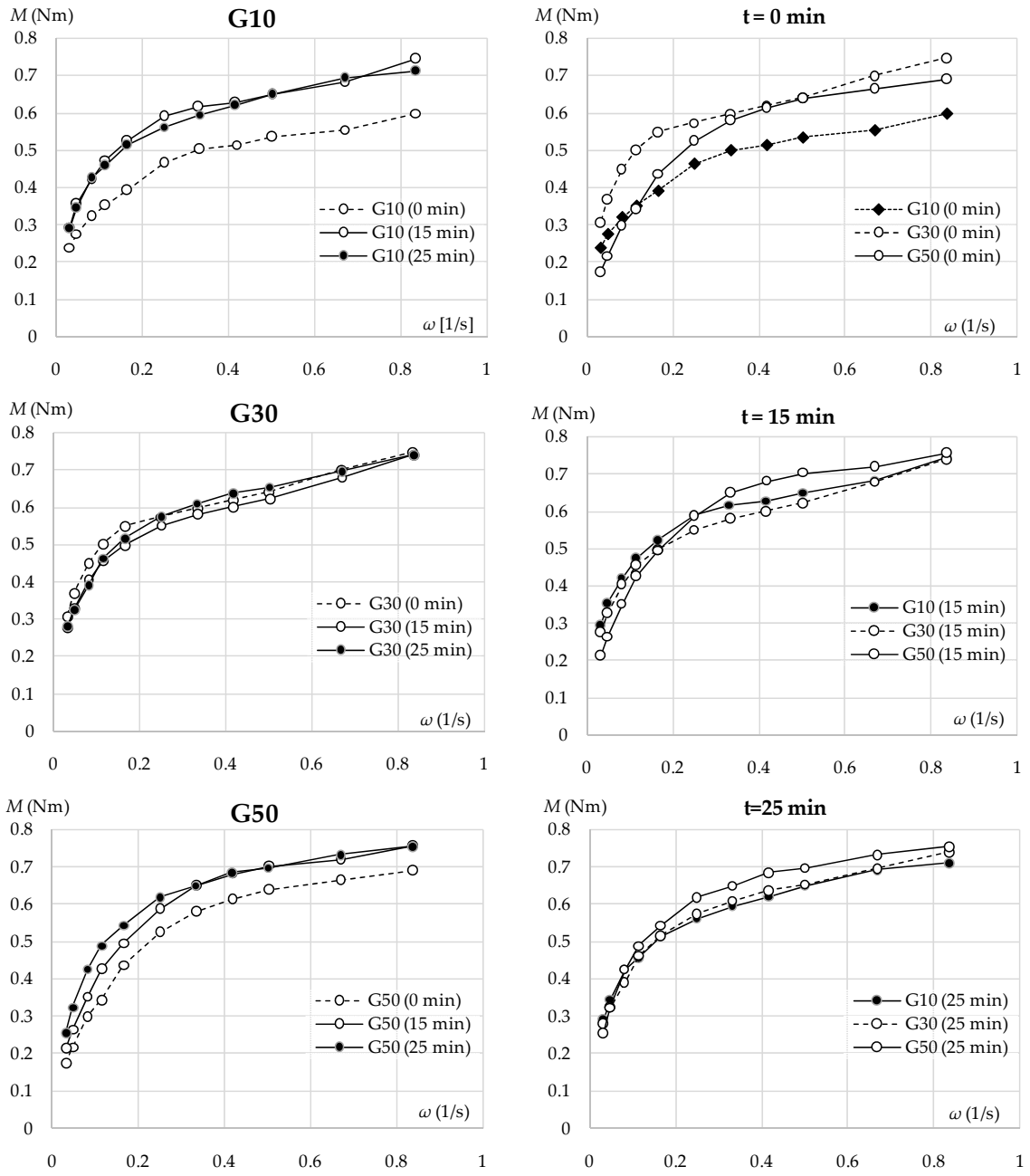


Figure 1. Flow curves for geopolymer mortars G10, G30 and G50.

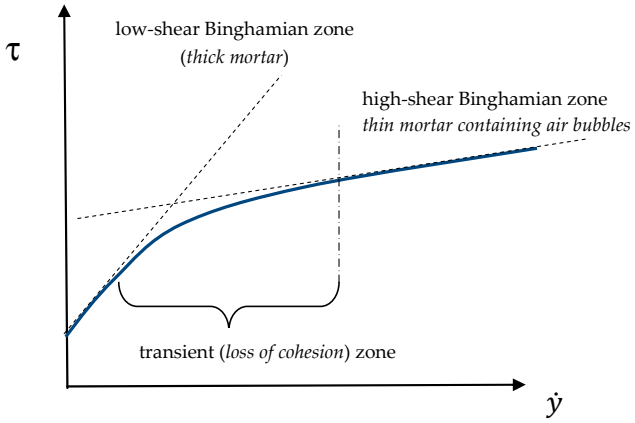


Figure 2. Flow model hypothesis.

Additionally, f/b (fluid-to-binder ratio) was around 0.45, i.e., much higher than the value needed to obtain shear-thickening behavior, typical, e.g., for self-compacting concrete [32]. That is why at low shear rates the tested mixes behaved like typical low-consistency thick cement paste or mortar (see e.g., [28]), i.e., following the Bingham model (i.e., $n = 1$ in Equation (1)) with a comparatively low yield value and high viscosity. At higher shear rates cohesion loss was observed, granular skeleton loosened and some air was entrapped. As a result torque lowering was registered (comparing to the linear response). At the certain shear rate this phenomenon stabilized (i.e., there was no significant additional cohesion loss observed). That is why the flow curve again became close to the straight line, but with a higher theoretical yield value and lower viscosity, like for low paste content mortar due to paste suction into air bubbles [28,33].

The second important observation is that consistency loss was taking place in two steps. The first step was occurring between 5 and 20 min after the finishing of mixing, and the second one around 35 min after mixing. The second step was neglected in rheological measurements due to problems with filling both viscometer vessel and forms used for sampling. The same problem occurred in the case of consistency measurement in the Haegermann flow table. All mixes were outside the method range (10/break results were obtained). According to Figure 1, left side, during the first step drop of consistence was caused mainly by the increase in viscosity in the low-shear zone, as defined in Figure 2. The high-shear zone was remaining almost unchanged. Judging from visual observations, in the second step the main consistency drop was probably associated with a yield value rise. In the case of G30 mix the first consistency drop was barely visible.

The right side of Figure 1 shows that after the first consistency drop all three geopolymers behaved similarly. The greatest difference was observed for the first test and the lowest for the last one. In the first test case the main difference was in low-shear zone viscosity. G10 mix had the lowest value of this parameter but it is also possible that all mixes had in fact both rheological parameters similar (except for lower yield value for G50 mix—see also Table 5) and the difference occurred only in the critical shear rate for transient zone appearance—in the G10 case (low slag content) this point was obtained at the lowest shear rate, i.e., cohesion was the weakest. Unfortunately, there was no possibility to repeat the tests due to a lack of spare material for mix preparation.

3.2. *The Effect of GGBFS Content on the Density and Strength of Geopolymer Mortar*

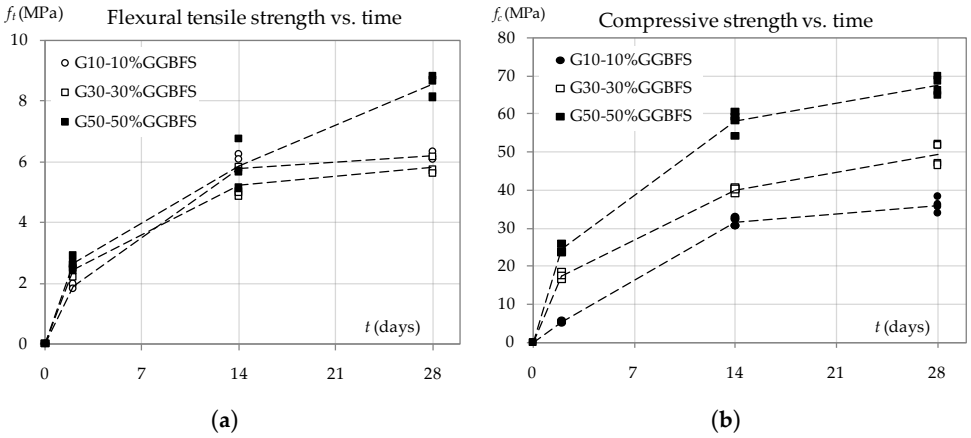
The results below show the apparent density obtained as well as the graphs of compressive and flexural tensile strength results after 2, 14 and 28 days. The apparent densities of geopolymer mortars G10, G30 and G50 are presented in Table 6. The maturing of the mortar samples is accompanied by material drying. The effect of the process was weight loss, which was recorded for all mortars. The change of mass is progressive, so the apparent density of the mortar changes as a function of time. It can be seen that a higher GGBFS content induced a density increase. In order to investigate

the porosity change and its characteristic, the pore size distribution was evaluated and presented in Section 3.3.

Table 6. Apparent densities of geopolymer mortars G10, G30 and G50 at different ages.

Mean Values of Apparent Density	G10 (kg/m^3)	G30 (kg/m^3)	G50 (kg/m^3)
2d	2093	2131	2223
14d	2051	2082	2211
28d	2048	2080	2207

The flexural tensile strength and compressive strength results for all geopolymer mortars G10, G30 and G50 are presented in Figure 3.



(**a**) (**b**)

Figure 3. (**a**) Flexural tensile strength and (**b**) compressive strength.

After 2 and 14 days, the development of flexural tensile strength (f_t) was similar for all materials. Clearly, higher values of f_t for G50 were observed after 28 days and reached 8.6 MPa. This effect can be associated with the development of geopolymer structures in a blended FA-GGBFS system. The compressive strength (f_c) after 2 days was 5.5 MPa, 17.5 MPa and 24.0 MPa respectively for the reference mortars G10, G30 and G50. The FA-GGBFS blended geopolymer mortars with higher GGBFS content presented better performances in compression Figure 3b. After 28 days the f_c values had reached 36.0 MPa, 49.5 MPa and 67.5 MPa respectively for G10, G30 and G50. The higher GGBFS contents give more of a compact structure of the material and resulted in better mechanical performances (see MIP results below).

The geopolymer structure, built of reaction products of aluminosilicates in an alkaline medium, is closely related to the precursor composition. In the case of blended systems containing FA class F and GGBFS, which additionally introduces calcium into the material structure, the mechanism of binding and determining the properties of the material is more complex. The hardened geopolymer contains both polymerization reaction products and unreacted precursor residues. The main product of the FA alkaline reaction is amorphous hydrated alkali-aluminosilicate (N-A-S-H) and for GGBFS it is calcium silicate hydrate (C-S-H) [34,35]. In addition, various reaction products of FA and GGBFS with an alkaline solution may interact with each other. In binders containing FA and GGBFS, the formation of hybrid C-N-A-S-H gels is observed [36]. The nature of the gel in fly ash-slag blended binders is strongly dependent on the slag/fly ash ratio. Differences in chemistry and mineralogy of precursors result in different binder products. The phase composition of a specific geopolymer binder determines the properties of the hardened material. Complete assessment of the impact of the precursor composition on the material properties obtained requires an analysis of the resulting geopolymer structures. According to Marjanović et al. [37], the reaction products of GGBFS in an alkaline medium result mainly in the

improvement of compressive strength. A higher amount of GGBFS in the geopolymer binder results in a denser structure and leads to a higher strength of hardened material [22]. Due to the high CaO content in GGBFS, it is possible to form C-S-H gel at an early stage [38]. The addition of GGBFS enhances the early properties of the FA-based geopolymer [39].

3.3. The Pore Size Distribution of Geopolymer Mortar by MIP

Total porosity was deducted from the cumulative intrusion of mercury pictograms presented in Figure 4. The pore size distribution of G10, G30 and G50 mortars at the age of 28 days obtained by MIP is presented in Figure 5. For each material two specimens were prepared.

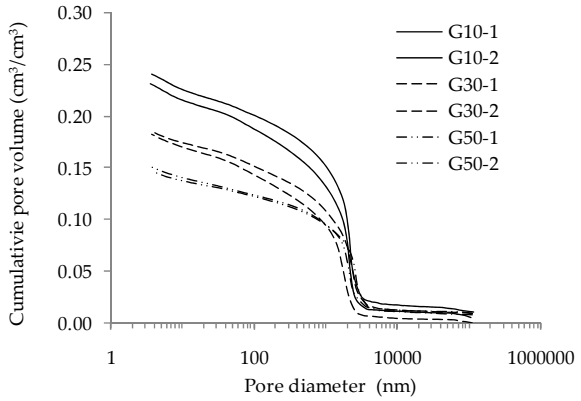


Figure 4. Cumulative pore volume and total porosity of FA-GGBFS blended geopolymers mortars by mercury intrusion porosimetry (MIP).

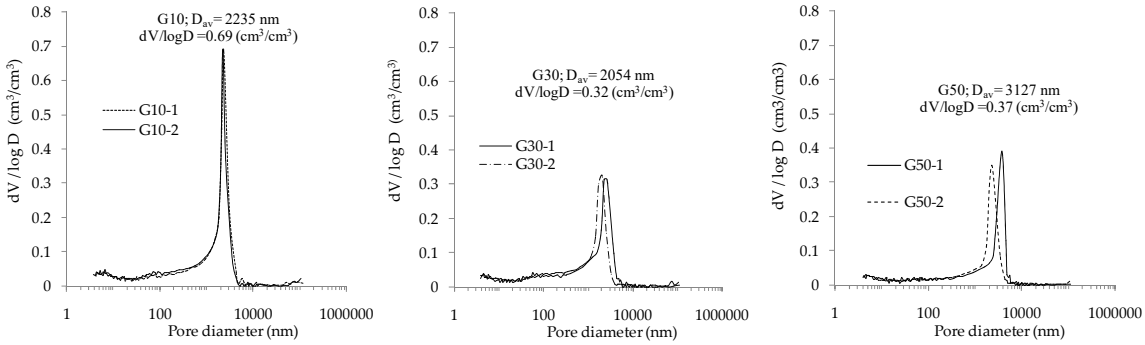


Figure 5. Pore size distribution of FA-GGBFS blended geopolymers mortars by MIP.

For geopolymer mortar samples G50-1 and G50-2 the results cumulative pore volume have shown that the total porosity of those materials reached the values of 0.145 and 0.144 cm^3/cm^3, which was 37% lower than for G10 mortars, which presented 0.227 and 0.237 cm^3/cm^3. The addition of higher content of GGBFS resulted in lower porosity and a denser structure.

All geopolymers mortars G10, G30 and G50 present a bell curve shape with a clear one peak situated on 2230 nm, 2054 nm and 3127 nm. The peak was particularly pronounced for samples with a 10 wt% addition of GGBFS. The results show that in the case of tested geopolymers mortars macropores (>50 nm) were dominant. In the literature, the pore size distribution of geopolymer hardened pastes (binder with no aggregates) is most often presented as a bell curve with the maximum in a region of mesopores [40–43]. In case of the potassium-based geopolymer paste a maximum value was situated within the range of 8–30 nm [43] or 7–10 nm [40,42,44]. In turn, sodium-based geopolymer paste had the peak shifted toward 30 nm [41,44]. In our study the sand presence had a influence on porosity and pore-size distribution that is why the results differ from those presenting pastes [40–43] where the dominant pores diameters were situated in lower values.

4. Conclusions

This study investigated fresh state rheological properties of blended FA-GGBFS geopolymer mortars in the time frame from 0–25 min. The impact of replacement of the FA by GGBFS in the amount of 10 wt%, 30 wt% and 50 wt% on the flow behavior in the fresh state and the mechanical performances of the hardened material were examined.

Based on the conducted research, it can be stated that the content of GGBFS in the range up to 50 wt% did not significantly alter the rheology of geopolymer mortars within the time rage from 0 to 25 min The increase in GGBFS content was accompanied by a decrease in consistency (i.e., an increase in yield stress), but the differences between the successive levels analyzed were not very significant.

The mortars tested were considered as multi-phase systems due to the presence of paste and filler in the form of fine aggregate. The analysis of the rheology of such mixes is particularly difficult, as the properties of the mixes are determined by different mechanisms and phenomena. In the case of the mortars under consideration, a relatively high content of paste can have a decisive effect on the rheological properties of the mixes. During the fresh mix tests, a consistency loss was perceived in two steps. The first step was occurring between 5 and 20 min. The drop inconsistency was caused mainly by the increase in viscosity in the low-shear zone. The second decrease around 35 min after mixing was observed and the consistency drop was probably associated to a yield value rise.

The analyses conducted indicate a certain analogy between the behavior of the geopolymer mortars to that of a pseudoplastic liquid representing shear thinning behavior. The flow curves obtained were highly non-linear, following roughly the Herschel–Bulkley model with $n < 1$. The relatively high paste to sand ratio and the presence of alkalis in the mix most probably have a decisive effect on the rheological properties of the tested materials, i.e., high viscosity, low yield value response in the low-shear zone. The observed shear thinning behavior results probably from the occurrence of reversible mortar aeration process in the mid-shear zone. In the high shear zone high but stable aeration occurs, resulting in the change of rheological response to high yield and low viscosity.

Tests of mechanical properties show a clear increase in strength together with an increase in the amount of GGBFS. After 28 days the f_c values had reached 36.0 MPa, 49.5 MPa and 67.5 MPa respectively for G10, G30 and G50. The higher GGBFS contents give a more compact structure of the material and the result is higher apparent densities and better mechanical properties. The total porosity measured with the MIP method have shown that the porosity of the fly ash geopolymer mortar with higher GGBFS addition gave a denser matrix with a total open porosity of 14%. The dominant diameter of the pores was located in the macropores region between 2050 and 3130 nm for all tested FA-GGBFS blended geopolymers mortars. The sand presence had a significant impact on porosity and pore-size distribution when comparing to the literature where geopolymer pastes were investigated.

The presented research results of rheology of geopolymer mortars can form the basis for further development works for use geopolymer mortars with blended FA-GGBFS binder in additive manufacturing (3D printing technology).

Author Contributions: Conceptualization, I.H. Data curation, M.S. and M.U. Funding acquisition, I.H. Investigation, M.S. and M.U. Methodology, M.U. Supervision, I.H. Validation, M.U. Writing—original draft, M.S., M.U. and I.H. Writing—review and editing, I.H. and M.S. All authors have read and agreed to the published version of the manuscript.

Funding: The study was financially supported by the EMMAT project, E-mobility and sustainable materials and technologies (PPI/APM/2018/1/00027) NAWA—The Polish National Agency For Academic Exchange.

Conflicts of Interest: The authors declare no conflict of interest.

References

1. Duxson, P.; Provis, J.L.; Lukey, G.C.; van Deventer, J.S.J. The role of inorganic polymer technology in the development of "green concrete". *Cem. Concr. Res.* **2007**, *37*, 1590–1597. [CrossRef]
2. Juenger, M.C.G.; Winnefeld, F.; Provis, J.L.; Ideker, J.H. Advances in alternative cementitious binders. *Cem. Concr. Res.* **2011**, *41*, 1232–1243. [CrossRef]

3. Hardjito, D.; Wallah, S.E.; Sumajouw, D.M.J.; Rangan, B.V. Factors Influencing The Compressive Strength of Fly Ash-Based Geopolymer Concrete. *Civ. Eng. Dimens.* **2007**, *6*, 88–93.
4. Fernández-Jiménez, A.; Puertas, F. Effect of activator mix on the hydration and strength behaviour of alkali-activated slag cements. *Adv. Cem. Res.* **2003**, *15*, 129–136. [CrossRef]
5. Bakharev, T.; Sanjayan, J.G.; Cheng, Y.B. Resistance of alkali-activated slag concrete to acid attack. *Cem. Concr. Res.* **2003**, *33*, 1607–1611. [CrossRef]
6. Barbosa, V.F.F.; MacKenzie, K.J.D. Thermal behaviour of inorganic geopolymers and composites derived from sodium polysialate. *Mater. Res. Bull.* **2003**, *38*, 319–331. [CrossRef]
7. Laskar, A.I.; Bhattacharjee, R. Effect of Plasticizer and Superplasticizer on Rheology of Fly-Ash-Based Geopolyrner Concrete. *ACI Mater. J.* **2013**, *110*, 513–518.
8. Romagnoli, M.; Leonelli, C.; Kamse, E.; Lassinantti Gualtieri, M. Rheology of geopolymer by DOE approach. *Constr. Build. Mater.* **2012**, *36*, 251–258. [CrossRef]
9. Romagnoli, M.; Sassatelli, P.; Lassinantti Gualtieri, M.; Tari, G. Rheological characterisation of fly ash-based suspensions. *Constr. Build. Mater.* **2014**, *65*, 526–534. [CrossRef]
10. Li, C.; Sun, H.; Li, L. A review: The comparison between alkali-activated slag (Si + Ca) and metakaolin (Si + Al) cements. *Cem. Concr. Res.* **2010**, *40*, 1341–1349. [CrossRef]
11. Oh, J.E.; Monteiro, P.J.M.; Jun, S.S.; Choi, S.; Clark, S.M. The evolution of strength and crystalline phases for alkali-activated ground blast furnace slag and fly ash-based geopolymers. *Cem. Concr. Res.* **2010**, *40*, 189–196. [CrossRef]
12. Bell, J.L.; Sarin, P.; Driemeyer, P.E.; Haggerty, R.P.; Chupas, P.J.; Kriven, W.M. X-Ray pair distribution function analysis of a metakaolin-based, $KAlSi_2O_6{\cdot}5.\ 5H_2O$ inorganic polymer (geopolymer). *J. Mater. Chem.* **2008**, *18*, 5974–5981. [CrossRef]
13. Meral, C.; Benmore, C.J.; Monteiro, P.J.M. The study of disorder and nanocrystallinity in C-S-H, supplementary cementitious materials and geopolymers using pair distribution function analysis. *Cem. Concr. Res.* **2011**, *41*, 696–710. [CrossRef]
14. Duxson, P.; Provis, J.L.; Lukey, G.C.; Mallicoat, S.W.; Kriven, W.M.; Van Deventer, J.S.J. Understanding the relationship between geopolymer composition, microstructure and mechanical properties. *Colloids Surf. A Physicochem. Eng. Asp.* **2005**, *269*, 47–58. [CrossRef]
15. Favier, A.; Habert, G.; D'Espinose De Lacaillerie, J.B.; Roussel, N. Mechanical properties and compositional heterogeneities of fresh geopolymer pastes. *Cem. Concr. Res.* **2013**, *48*, 9–16. [CrossRef]
16. Favier, A.; Hot, J.; Habert, G.; d'Espinose de Lacaillerie, J.-B.; Roussel, N. Rheology of geopolymer: Comparative study between portland cement and metakaolin based geopolymer. In Proceedings of the 1st RILEM International Conference on Rheology and Processing of Construction Materials, Paris, France, 2–4 September 2013.
17. Flatt, R.J. Towards a prediction of superplasticized concrete rheology. *Mater. Struct. Constr.* **2004**, *37*, 289–300. [CrossRef]
18. Paper, C.; Habert, G.; Zurich, E.T.H. Rheology of metakaolin based geopolymer: Mechanisms and improvement potentials 2. In Proceedings of the Twelfth International Conference on Recent Advances in Concrete Technology and Sustainability Issues, Prague, Czech Republic, 30 October–2 November 2012.
19. Duxson, P.; Provis, J.L. Designing precursors for geopolymer cements. *J. Am. Ceram. Soc.* **2008**, *91*, 3864–3869. [CrossRef]
20. Panda, B.; Unluer, C.; Tan, M.J. Investigation of the rheology and strength of geopolymer mixtures for extrusion-based 3D printing. *Cem. Concr. Compos.* **2018**, *94*, 307–314. [CrossRef]
21. Favier, A.; Hot, J.; Habert, G.; Roussel, N.; D'Espinose De Lacaillerie, J.B. Flow properties of MK-based geopolymer pastes. A comparative study with standard Portland cement pastes. *Soft Matter* **2014**, *10*, 1134–1141. [CrossRef]
22. Saha, S.; Rajasekaran, C. Enhancement of the properties of fly ash based geopolymer paste by incorporating ground granulated blast furnace slag. *Constr. Build. Mater.* **2017**, *146*, 615–620. [CrossRef]
23. Roussel, N.; Lemaître, A.; Flatt, R.J.; Coussot, P. Steady state flow of cement suspensions: A micromechanical state of the art. *Cem. Concr. Res.* **2010**, *40*, 77–84. [CrossRef]
24. Zhang, D.-W.; Wang, D.; Liu, Z.; Xie, F. Rheology, agglomerate structure, and particle shape of fresh geopolymer pastes with different NaOH activators content. *Constr. Build. Mater.* **2018**, *187*, 674–680. [CrossRef]

25. Zhang, D.-W.; Wang, D.; Lin, X.-Q.; Zhang, T. The study of the structure rebuilding and yield stress of 3D printing geopolymer pastes. *Constr. Build. Mater.* **2018**, *184*, 575–580. [CrossRef]
26. Davidovits, J. *Geopolymer Chemistry and Applications*, 4th ed.; Geopolymer Institute: Saint-Quentin, France, 2015; ISBN 9782951482050.
27. Urban, M. Consistency measures of self compacting concrete and its rheological parameters. In Proceedings of the 16, Ibausil, Weimar, Germany, 20–23 September 2006; Volume 2, pp. 131–138.
28. Tattersall, G.; Banfill, P.F.G. *The Rheology of Fresh Concrete*; Pitman: Belfast, UK, 1983.
29. Giesche, H. Mercury Porosimetry. In *Handbook of Porous Solids*; John Wiley & Sons, Ltd.: Hoboken, NJ, USA, 2008; pp. 309–351; ISBN 9783527618286.
30. Szwabowski, J. Influence of three-phase structure on the yield stress of fresh concrete. In *Rheology of Fresh Cement and Concrete*; Taylor & Francis: London, UK, 2010; pp. 241–248.
31. Schwartzentruber, A.; Catherine, C. Method of the concrete equivalent mortar (CEM)—A new tool to design concrete containing admixture. *Mater. Struct. Constr.* **2000**, *33*, 475–482. [CrossRef]
32. De Schutter, G.; Gibbs, J.; Domone, P.; Bartos, P.J.M. *Self-Compacting Concrete*; Whittles Publishing: Scotland, UK, 2008; ISBN 1904445306.
33. Wallevik, O.; Níelsson, I. Rheological evaluation of some empirical test methods-preliminary results. In Proceedings of the Third International Symposium on Self-compacting Concrete, Reykjavik, Iceland, 17–20 August 2003; RILEM: Reykjavik, Iceland, 2003; p. 1028.
34. Khale, D.; Chaudhary, R. Mechanism of Geopolymerization and Factors Influencing Its Development: A Review. *J. Mater. Sci.* **2007**, *42*, 729–746. [CrossRef]
35. Duxson, P.; Fernández-Jiménez, A.; Provis, J.L.; Lukey, G.C.; Palomo, A.; Van Deventer, J.S.J. Geopolymer technology: The current state of the art. *J. Mater. Sci.* **2007**, *42*, 2917–2933. [CrossRef]
36. Ismail, I.; Bernal, S.A.; Provis, J.L.; San Nicolas, R.; Hamdan, S.; Van Deventer, J.S.J. Modification of phase evolution in alkali-activated blast furnace slag by the incorporation of fly ash. *Cem. Concr. Compos.* **2014**, *45*, 125–135. [CrossRef]
37. Marjanović, N.; Komljenović, M.; Baščarević, Z.; Nikolić, V.; Petrović, R. Physical–mechanical and microstructural properties of alkali-activated fly ash–blast furnace slag blends. *Ceram. Int.* **2015**, *41*, 1421–1435. [CrossRef]
38. Singh, N.B.; Middendorf, B. Geopolymers as an alternative to Portland cement: An overview. *Constr. Build. Mater.* **2020**, *237*, 117455. [CrossRef]
39. Shang, J.; Dai, J.G.; Zhao, T.J.; Guo, S.Y.; Zhang, P.; Mu, B. Alternation of traditional cement mortars using fly ash-based geopolymer mortars modified by slag. *J. Clean. Prod.* **2018**, *203*, 746–756. [CrossRef]
40. Rovnaník, P. Effect of curing temperature on the development of hard structure of metakaolin-based geopolymer. *Constr. Build. Mater.* **2010**, *24*, 1176–1183. [CrossRef]
41. Steins, P.; Poulesquen, A.; Frizon, F.; Diat, O.; Jestin, J.; Causse, J.; Lambertin, D.; Rossignol, S. Effect of aging and alkali activator on the porous structure of a geopolymer. *J. Appl. Crystallogr.* **2014**, *47*, 316–324. [CrossRef]
42. Kong, D.L.Y.; Sanjayan, J.G.; Sagoe-Crentsil, K. Comparative performance of geopolymers made with metakaolin and fly ash after exposure to elevated temperatures. *Cem. Concr. Res.* **2007**, *37*, 1583–1589. [CrossRef]
43. Medpelli, D.; Seo, J.-M.; Seo, D.-K. Geopolymer with Hierarchically Meso-/Macroporous Structures from Reactive Emulsion Templating. *J. Am. Ceram. Soc.* **2014**, *97*, 70–73. [CrossRef]
44. Boher, C.; Martin, I.; Lorente, S.; Frizon, F. Experimental investigation of gas diffusion through monomodal materials. Application to geopolymers and Vycor® glasses. *Microporous Mesoporous Mater.* **2014**, *184*, 28–36. [CrossRef]



© 2020 by the authors. Licensee MDPI, Basel, Switzerland. This article is an open access article distributed under the terms and conditions of the Creative Commons Attribution (CC BY) license (http://creativecommons.org/licenses/by/4.0/).